Effects of elastic anisotropy on primary petroleum migration through buoyancy-driven crack propagation

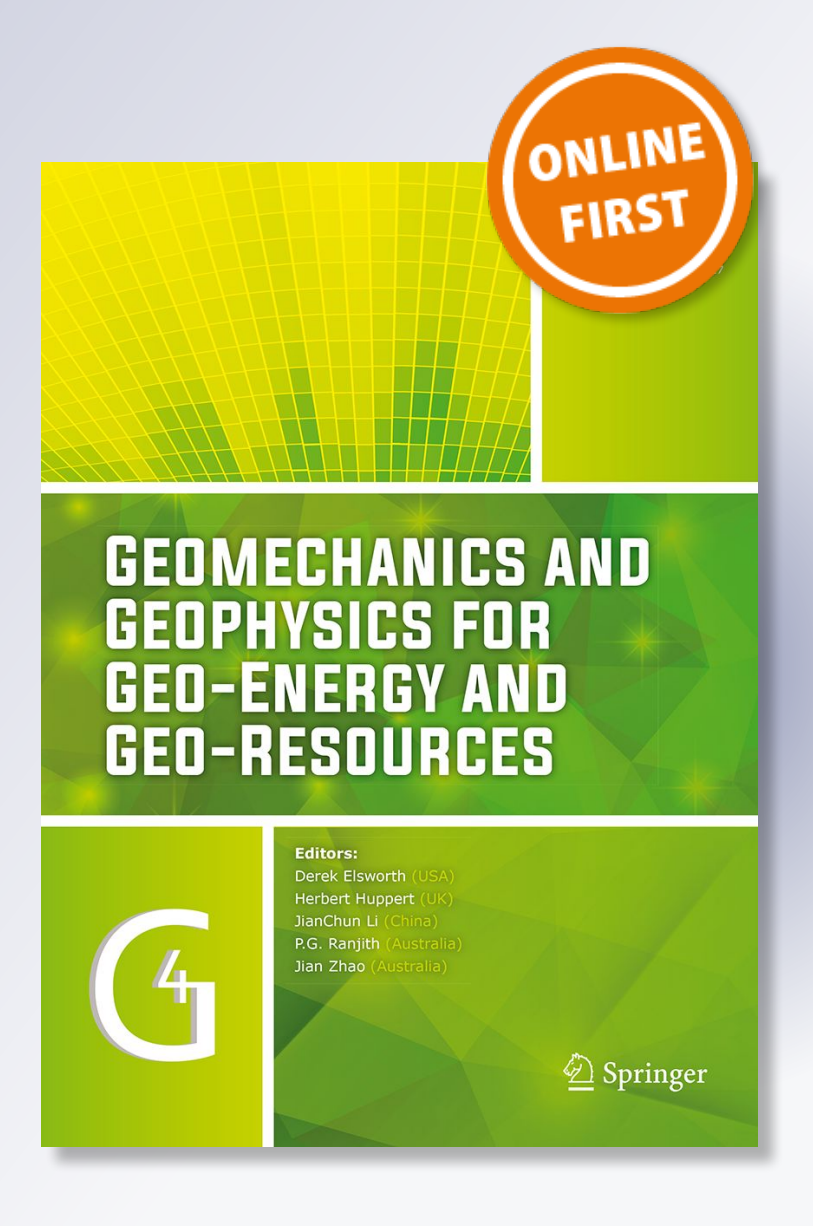
Z.-H. Jin & S. E. Johnson

Geomechanics and Geophysics for Geo-Energy and Geo-Resources

ISSN 2363-8419

Geomech. Geophys. Geo-energ. Georesour.

DOI 10.1007/s40948-017-0062-6





Your article is protected by copyright and all rights are held exclusively by Springer International Publishing Switzerland. This eoffprint is for personal use only and shall not be self-archived in electronic repositories. If you wish to self-archive your article, please use the accepted manuscript version for posting on your own website. You may further deposit the accepted manuscript version in any repository, provided it is only made publicly available 12 months after official publication or later and provided acknowledgement is given to the original source of publication and a link is inserted to the published article on Springer's website. The link must be accompanied by the following text: "The final publication is available at link.springer.com".



Geomech. Geophys. Geo-energ. Geo-resour. DOI 10.1007/s40948-017-0062-6

ORIGINAL ARTICLE



Effects of elastic anisotropy on primary petroleum migration through buoyancy-driven crack propagation

Z.-H. Jin · S. E. Johnson

Received: 12 January 2017 / Accepted: 28 April 2017 © Springer International Publishing Switzerland 2017

Abstract Material anisotropy may significantly influence the behavior of fluid transport in sedimentary basins and other environments with laminated or foliated rocks. In this paper, we present a fracture mechanics model to investigate primary migration of petroleum (oil and gas) through propagation of a vertical, buoyancy-driven blade crack in a transversely isotropic source rock. The source rock is assumed to have very low permeability and hence can be modeled as a linear elastic medium. Fracture parameters (stress intensity factor and crack opening displacement) are derived using an equivalent set of anisotropic elastic properties. The crack propagation velocity (i.e., petroleum migration velocity) and crack opening (fracture aperture) are determined using a fracture mechanics criterion together with the first order approximation of plane Poiseuille flow equations of fluid mechanics. For subhorizontal layering, we find that the fluid migration velocity and fracture aperture are significantly increased if the elastic modulus in the vertical direction is smaller than that in the horizontal direction. Finally, we discuss the applicability of the formula for isotropic materials along with the equivalent anisotropic elastic parameters introduced in this paper to evaluate fracture aperture for cracks in anisotropic rocks.

Keywords Fluid-filled crack · Crack propagation · Primary petroleum migration · Anisotropy · Buoyancy

1 Introduction

Primary migration of petroleum is a process in which oil and natural gas formed in the source rock are transported from the source region to overlying carrier rocks (Mann 1990; Hunt 1996). Several mechanisms have been proposed for primary petroleum migration in the source rock. These mechanisms include porous fluid flow, molecular diffusion, and fracture permeability (Mann 1990). Petroleum source rocks are typically organic-rich shale characterized by extremely low permeability, which renders porous flow governed by Darcy's law an unsatisfactory explanation for primary migration in many instances, particularly where flow must occur across a strongly laminated microfabric. Molecular diffusion and migration in solution with water are typically considered as negligible contributors owing to the low solubility of oil in water (England et al. 1987; Hunt 1996). Fracture permeability, on the other hand, has been considered as the most likely mechanism for primary petroleum migration (e.g., Palciauskas and

Z.-H. Jin (⊠)

Department of Mechanical Engineering, University of Maine, Orono, ME 04469, USA e-mail: zhihe.jin@maine.edu

S. E. Johnson School of Earth and Climate Sciences, University of Maine, Orono, ME 04469, USA

Published online: 12 May 2017



Domenico 1980; Comer and Hinch 1987; Hunt 1990; Miller 1995; Law and Spencer 1998; Nelson 2001; Lash and Engelder 2005), which is supported by the existence of bitumen-filled cracks found in samples from source rocks (e.g., Comer and Hinch 1987; Hunt 1990; Mann 1990; Nelson 2001; Lash and Engelder 2005).

In this paper we examine primary petroleum migration through crack propagation and in particular the effect of host-rock anisotropy on the velocity and physical dimensions of a mobile crack filled by oil or gas ascending vertically through flat-lying, transversely isotropic rocks. Primary petroleum migration through fractures is generally driven by overpressures that are generated in the petroleum source region, buoyancy forces due to the density differences between the host rock and petroleum in the crack, or a combination of overpressure and buoyancy force.

Weertman (1971) first studied buoyancy-driven propagation of an isolated, water-filled vertical crack. During crack propagation the upper tip continuously moves up as the rock is fractured and the lower crack tip closes. Nunn (1996) considered propagation of an oil-filled fracture and calculated the fracture propagation velocity using a first order approximation of Poiseuille flow model. Nunn and Meulbroek (2002) further studied propagation of a crack filled by methane gas and considered the effects of gas viscosity and compressibility on the gas migration velocity. Jin and Johnson (2008) investigated the effect of crack interaction on the fracture propagation velocity and hence oil flux by considering multiple parallel, oil-filled cracks. Jin et al. (2015) examined the stability of a crack filled with methane and water formed by dissociation of methane hydrates in lowpermeability marine muds. Besides cracks filled by water, oil and gas, magma-filled isolated cracks have also been studied. Dahm (2000a) simulated propagation direction of magma-filled fractures using a boundary element method. Dahm (2000b) also discussed the shape and velocity for ascending fractures filled by water, oil and magma. Roper and Lister (2007) examined evolution of an isolated magmafilled void from an initial elliptical shape to a cracklike shape. Finally, Pan et al. (2014) simulated interaction of CO₂-filled cracks using a numerical cellular automata method.

The existing studies on buoyancy-driven propagation of fluid-filled cracks assume that the host rock is an isotropic medium. In general, petroleum source rocks are anisotropic, i.e., their properties are direction-dependent. For example, in laminated sedimentary rocks (including shale) the elastic modulus usually does not vary significantly within the bedding plane. However, the modulus perpendicular to the bedding plane is typically lower than that in the bedding plane although the opposite can also occur in some cases (Amadei and Pan 1992). Such sedimentary rocks are usually modeled as transversely isotropic media with the bedding plane as the transversely isotropic plane (Bayuk et al. 2008; Nihei et al. 2011). The anisotropy of petroleum source rocks may increase or decrease the velocity of petroleum migration through fractures because the velocity is proportional to the square of the average fracture aperture (Nunn 1996), which is influenced by the material anisotropy.

The present work investigates the effect of elastic anisotropy of a host rock on petroleum migration through buoyancy-driven fracture propagation. As far as we are aware, the effects of elastic anisotropy on buoyancy-driven propagation of fluid-fill fractures have not previously been investigated. We assume that the host rock is transversely isotropic in the bedding plane and has very low permeability. For the purposes of the current analysis, we also assume that the bedding plane is horizontal, although the method can be extended to any orientation of transverse anisotropy. The host rock thus can be modeled as a linearly elastic, transversely isotropic medium. This assumption is reasonable for shale petroleum source rocks as well as a broad range of foliated metamorphic rocks. We note that cracks in general anisotropic rocks have been investigated using both analytical and numerical methods (e.g., Pan and Amadei 1996; Pan 1997; Chen et al. 1998; Pan and Yuan 2000; Pan and Chen 2015). The numerical methods developed in those works can also be used to solve problems of cracks in arbitrary orientations in an anisotropic rock. The present work focuses on coupling between crack propagation and petroleum migration and use of an equivalent set of elastic parameters to investigate the effect of elastic anisotropy of source rocks on primary petroleum migration.

We consider a single blade crack filled by oil or gas propagating in the vertical direction in the host source rock. We first introduce the basic equations of transversely isotropic elasticity and present an



equivalent set of anisotropic material parameters. This is the first application of these equivalent anisotropic parameters in geophysics as far as we know. We then use an integral equation method to solve the basic anisotropic elasticity equations in terms of the equivalent material parameters and derive the expressions for crack propagation velocity and crack opening displacement (i.e., fracture aperture). Numerical results for migration of oil, methane gas and water are presented to quantitatively illustrate the effect of elastic anisotropy on the propagation velocity and crack opening displacement.

2 Transversely isotropic elasticity

We consider vertical propagation of an isolated, fluid-filled blade crack in a transversely isotropic host rock. The isotropic plane is horizontal (*x*–*y* plane) in which the elastic properties are the same in all in-plane directions. The Young's modulus in the vertical direction (*z*-direction) differs from that in the isotropic plane. The constitutive equations are as follows

$$\varepsilon_{xx} = \frac{1}{E_h} \sigma_{xx} - \frac{v_{hh}}{E_h} \sigma_{yy} - \frac{v_{vh}}{E_v} \sigma_{zz},
\varepsilon_{yy} = -\frac{v_{hh}}{E_h} \sigma_{xx} + \frac{1}{E_h} \sigma_{yy} - \frac{v_{vh}}{E_v} \sigma_{zz},
\varepsilon_{zz} = -\frac{v_{vh}}{E_v} \sigma_{xx} - \frac{v_{vh}}{E_v} \sigma_{yy} + \frac{1}{E_v} \sigma_{zz},
\varepsilon_{xy} = \frac{1}{2G_{hh}} \sigma_{xy}, \quad \varepsilon_{yz} = \frac{1}{2G_{vh}} \sigma_{yz}, \quad \varepsilon_{zx} = \frac{1}{2G_{vh}} \sigma_{zx}$$
(1)

where σ_{ij} denotes stresses (i, j = x, y, z), ε_{ij} strains, $E_{\rm h}$ and $E_{\rm v}$ the Young's moduli in the isotropic plane and its perpendicular direction, respectively, $v_{\rm hh}$ and $v_{\rm vh}$ the Poisson's ratios in the isotropic plane and the x–z (or y–z) plane, respectively, $G_{\rm hh}$ and $G_{\rm vh}$ the shear moduli in the isotropic plane and the x–z (or y–z) plane, respectively. Finally, the shear modulus $G_{\rm hh}$ is not independent and is given by

$$G_{hh} = \frac{E_h}{2(1+v_{hh})}$$

For plane strain in the *x*–*z* plane, i.e., $\varepsilon_{yy} = \varepsilon_{yz} = \varepsilon_{xy} = 0$, the second equation in Eq. (1) gives

$$\sigma_{yy} = v_{hh}\sigma_{xx} + \frac{E_h}{E_{xy}}v_{vh}\sigma_{zz} \tag{2}$$

Substituting the equation above into Eq. (1) gives the following stress–strain relations in plane strain

$$\varepsilon_{xx} = \frac{1}{E'_h} \sigma_{xx} - \frac{1}{E'_{vh}} \sigma_{zz},$$

$$\varepsilon_{zz} = -\frac{1}{E'_{vh}} \sigma_{xx} + \frac{1}{E'_v} \sigma_{zz},$$

$$\gamma_{zx} = \frac{1}{G'_{vh}} \sigma_{zx}$$
(3)

where $\gamma_{zx} = 2\varepsilon_{zx}$ and

$$\frac{1}{E'_{h}} = \frac{1}{E_{h}} (1 - v_{hh} v_{hh}),$$

$$\frac{1}{E'_{v}} = \frac{1}{E_{v}} (1 - v_{hv} v_{vh}),$$

$$\frac{1}{E'_{vh}} = \frac{v_{vh}}{E_{v}} (1 + v_{hh}),$$

$$G'_{vh} = G_{vh}$$
(4)

in which v_{hv} and v_{vh} are related by

$$\frac{v_{hv}}{E_h} = \frac{v_{vh}}{E_v} \tag{5}$$

 $v_{\rm hv}$ represents contraction in the vertical direction due to horizontal tension whereas $v_{\rm vh}$ represents contraction in the horizontal direction due to vertical tension. The inverse form of Eq. (3) is

$$\sigma_{zz} = \frac{E'_{\nu}E'_{\nu h}E'_{\nu h}}{E'_{\nu h}E'_{\nu h} - E'_{h}E'_{\nu}} \left(\frac{E'_{h}}{E'_{\nu h}} \frac{\partial u_{x}}{\partial x} + \frac{\partial u_{z}}{\partial z}\right),$$

$$\sigma_{xx} = \frac{E'_{h}E'_{\nu h}E'_{\nu h}}{E'_{\nu h}E'_{\nu h} - E'_{h}E'_{\nu}} \left(\frac{\partial u_{x}}{\partial x} + \frac{E'_{\nu}}{E'_{\nu h}} \frac{\partial u_{z}}{\partial z}\right),$$

$$\sigma_{zx} = G'_{\nu h} \left(\frac{\partial u_{z}}{\partial x} + \frac{\partial u_{x}}{\partial z}\right)$$
(6)

where the following strain-displacement relations are used

$$\varepsilon_{zz} = \frac{\partial u_z}{\partial z}, \quad \varepsilon_{xx} = \frac{\partial u_x}{\partial x}, \quad \gamma_{zx} = \frac{\partial u_x}{\partial z} + \frac{\partial u_z}{\partial x}$$
 (7)

in which u_z and u_x are the displacements in the z- and x-directions, respectively.

Following Krenk (1979), we introduce the following material parameters



$$E_{0} = \sqrt{E'_{h}E'_{v}}, \quad v_{0} = \frac{\sqrt{E'_{h}E'_{v}}}{E'_{vh}}, \quad \lambda^{4} = \frac{E'_{v}}{E'_{h}}, \\ \kappa = \frac{E_{0}}{2G'_{vh}} - v_{0}$$
(8)

and the transformations for coordinates, displacements, and stresses

$$z_{1} = z/\sqrt{\lambda}, \quad z_{2} = x\sqrt{\lambda}$$

$$u_{1} = u_{z}\sqrt{\lambda}, \quad u_{2} = u_{x}/\sqrt{\lambda}$$

$$\tau_{11} = \sigma_{zz}/\lambda, \quad \tau_{22} = \lambda\sigma_{xx}, \quad \tau_{12} = \sigma_{zx}(\kappa + \nu_{0})/(1 + \nu_{0})$$
(9)

Now the constitutive relation in Eq. (6) can be written in the following simplified form similar to that for isotropic materials with "modulus" E_0 and "Poisson's ratio" v_0

$$\tau_{11} = \frac{E_0}{1 - v_0^2} \left(\frac{\partial u_1}{\partial z_1} + v_0 \frac{\partial u_2}{\partial z_2} \right),
\tau_{22} = \frac{E_0}{1 - v_0^2} \left(\frac{\partial u_2}{\partial z_2} + v_0 \frac{\partial u_1}{\partial z_1} \right),
\tau_{12} = \frac{E_0}{2(1 + v_0)} \left(\frac{\partial u_1}{\partial z_2} + \frac{\partial u_2}{\partial z_1} \right)$$
(10)

The equilibrium equations in terms of stresses σ_{zz} , σ_{xx} and σ_{zx} , and the transformed stresses $\tau_{\alpha\beta}$ (α , $\beta=1,2$) are

$$\begin{split} \frac{\partial \sigma_{zz}}{\partial z} + \frac{\partial \sigma_{zx}}{\partial x} &= 0, \\ \frac{\partial \sigma_{zx}}{\partial z} + \frac{\partial \sigma_{xx}}{\partial x} &= 0 \end{split} \tag{11a}$$

and

$$\frac{\partial \tau_{11}}{\partial z_1} + \frac{(1+\nu_0)}{(\kappa+\nu_0)} \frac{\partial \tau_{12}}{\partial z_2} = 0,$$

$$\frac{(1+\nu_0)}{(\kappa+\nu_0)} \frac{\partial \tau_{12}}{\partial z_1} + \frac{\partial \tau_{22}}{\partial z_2} = 0$$
(11b)

respectively. Substituting the transformed stresses in Eq. (10) into Eq. (11b), we have the governing equation for the transformed displacements as follows

$$\beta_{1} \frac{\partial^{2} u_{1}}{\partial z_{1}^{2}} + \frac{\partial^{2} u_{1}}{\partial z_{2}^{2}} + \beta_{2} \frac{\partial^{2} u_{2}}{\partial z_{1} \partial z_{2}} = 0,$$

$$\frac{\partial^{2} u_{2}}{\partial z_{1}^{2}} + \beta_{1} \frac{\partial^{2} u_{2}}{\partial z_{2}^{2}} + \beta_{2} \frac{\partial^{2} u_{1}}{\partial z_{1} \partial z_{2}} = 0$$
(12)

where β_1 and β_2 are constants given by



$$\beta_1 = 2(\kappa + \nu_0) / (1 - \nu_0^2),$$

$$\beta_2 = \nu_0 \beta_1 + 1$$
(13)

Parameters E_0 , v_0 , λ and κ are an equivalent set of elastic properties for transversely isotropic rocks undergoing plane strain deformations in the xz plane. Equations (8) to (10) are equivalent to those for orthotropic composites introduced by Krenk (1979). By using these parameters and the transformations in Eq. (9), the governing equations for the displacements of anisotropic materials are significantly simplified, which is convenient for obtaining closed-form solutions. Moreover, the similarity between the transformed constitutive relation (10) and that for isotropic materials allows examinations of using the equations for isotropic materials with the equivalent elastic properties to get approximate solutions of more complex problems of anisotropic materials.

3 A fluid-driven fracture propagation model

During the buoyancy-driven vertical propagation of an isolated fluid-filled crack, the fluid flows upward along the propagating fracture surfaces. The fluid pressure on the crack surfaces may be related to the crack opening displacement using the Poiseuville flow equations in fluid mechanics as follows (Spence et al. 1987; Roper and Lister 2007)

$$\frac{\partial \delta}{\partial t} = \frac{1}{12\eta} \frac{\partial}{\partial Z} \left[\delta^3 \left(\frac{\partial p_e}{\partial Z} - \Delta \rho g \right) \right] \tag{14}$$

where $p_{\rm e}$ is the excess pressure on the crack surfaces, δ the crack opening displacement, η the fluid viscosity, $\Delta \rho = \rho_{\rm rock} - \rho_{\rm fluid}$, $\rho_{\rm rock}$ the rock density, $\rho_{\rm fluid}$ the fluid density, g the gravitational acceleration, and Z a fixed vertical coordinate. Consider a special case of steady state crack propagation for which the crack opening profile does not change as observed in the moving coordinate attached to the crack (Spence et al. 1987; Lister 1991). Equation (14) now becomes (Spence et al. 1987; Chen et al. 2007)

$$-V\frac{\partial \delta}{\partial z} = \frac{1}{12\eta}\frac{\partial}{\partial z} \left[\delta^3 \left(\frac{\partial p_e}{\partial z} - \Delta \rho g \right) \right]$$
 (15)

where V is the crack propagation speed and z the moving vertical coordinate with the origin at the crack

center, i.e., the lower and upper crack tips are at z=-a and z=a, respectively, where a is the half crack length (Fig. 1). Integrate Eq. (15) twice to obtain

$$p_e(z) = p_e(0) + \Delta \rho gz - 12\eta V \int_{0}^{z} \delta^{-2} dz$$
 (16)

Using Taylor series expansion for the integral in the equation above we obtain the first order approximation of the excess pressure as follows

$$p_e(z) = p_e(0) + \left[\Delta \rho g - \frac{12\eta V}{\delta^2(0)}\right] z. \tag{17}$$

The fluid pressure in Eq. (17) is an equivalent form of the assumption adopted by Weertman (1971), Nakashima (1993) and Nunn (1996). A more general form of Eq. (17) consistent with that of Nunn (1996) can be written as

$$p_e = p_0 + p_1 z (18)$$

where p_0 is the excess pressure at the crack center (z = 0) and p_1 the excess pressure gradient. Equation (17) reduces to that for a stationary crack when the velocity V goes to zero. For the linear pressure distribution in Eqs. (18) or (17) to be reasonably accurate for propagating cracks, the viscous flow induced pressure drop must be much smaller than the

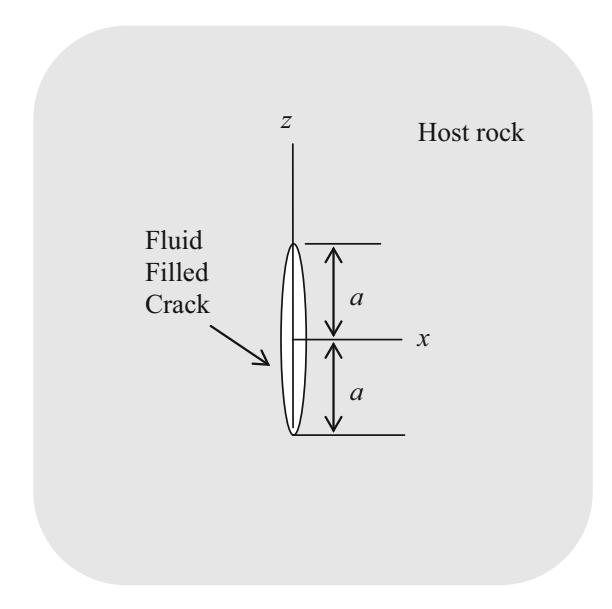


Fig. 1 A fluid-filled crack in the vertical z-direction

buoyancy force due to the density difference between the host rock and fluid, i.e., $12\eta Va/\delta^2(0)$ or $12\eta Va/\delta^2_{ave}$ should be much smaller than $\Delta\rho ga$, where δ_{ave} is the average crack opening. This condition will be examined using the numerical examples in the following Sect. 5.

While the linear pressure distribution may be a reasonable approximation of fluid pressure under the restricted condition discussed above, the argument is based on a steady state crack propagation condition. Steady state propagation has been adopted in a number of investigations in magma driven crack propagation (e.g., Spence et al. 1987; Lister 1991; Roper and Lister 2007; Chen et al. 2007) and oil/water migration through propagating fractures (Nakashima 1993; Nunn 1996; Jin and Johnson 2008). Roper and Lister (2007) presented a steady state propagation solution for a magma-filled semi-infinite crack. They also examined evolution of an isolated magma-filled void from an initial elliptical shape to a crack-like shape. They concluded that the crack opening profile in the head region approaches that for a steady state propagating semi-infinite crack while the lower crack tip remains stationary. Although upward propagation of the entire crack (i.e., the lower tip also moves) was not discussed in Roper and Lister (2007), their results indicated that the crack opening profile may remain approximately steady after the crack reaches its critical length and starts to propagate upward during which the lower tip closes and the crack length remains constant. For a gas-filled crack, although the crack length increases during crack propagation, substantial crack length increase occurs only over large propagation distances (the numerical example in Sect. 5 shows that a 4 m long crack at 4000 m depth increases to 4.6 m when the crack propagates to 2000 m depth). Hence, approximate steady state condition may still prevail.

In this study, we use the linear pressure distribution in Eq. (18) to examine the effects of rock anisotropy on the behavior of fluid migration through steady crack propagation. The pressure at the crack center p_0 and the pressure gradient p_1 are determined by the conditions that the upper crack tip propagates critically in the host rock and the lower crack tip closes during propagation. In linear elastic fracture mechanics, these conditions are described by

$$K_I(a) = K_{Ic}, \quad K_I(-a) = 0$$
 (19)



where $K_{\rm I}(a)$ and $K_{\rm I}(-a)$ are the stress intensity factors at the upper and lower tips, respectively, and $K_{\rm Ic}$ the fracture toughness of the host rock for crack propagation in the vertical direction. The pressure parameters p_0 and p_1 can be determined using the condition (19) once the stress intensity factors are obtained using fracture mechanics. The condition $K_{\rm I}(-a)=0$ in Eq. (19) at the closing lower crack tip may be reasoned as follows. First, $K_{\rm I}(-a)$ cannot be negative because a negative $K_{\rm I}$ means crack surface interpenetration in the near tip region. Second, if $K_{\rm I}(-a) > 0$, the lower crack tip is still open and will not move when the upper tip moves upward. Hence the crack length becomes longer which corresponds to a larger crack area as $K_{\rm I}$ remains $K_{\rm Ic}$ at the upper tip and the crack opening profile remains similar in steady state crack propagation. The larger crack area implies significant fluid flow into the crack from the host rock (to maintain the crack volume in the incompressible liquid case and to maintain the pressure in the compressible gas case), which contradicts the assumption of effectively impermeable host rock.

Figure 1 shows a vertical section (in the x–z plane) of a fluid-filled vertical blade crack where 2a is the length of the crack in the vertical direction. We assume that the size of the crack in the perpendicular direction to the x–z plane (y-direction) is relatively large so that a two-dimensional (2D) plane strain model (Nunn 1996; Bai and Pollard 2001) may be used.

A singular integral equation method is used to simulate propagation of the fluid-filled crack. The transformed Eqs. (10) and (12) and the equivalent elastic parameters E_0 , v_0 , λ and κ are used to solve the crack problem. The boundary conditions in terms of the transformed quantities are formulated as follows

$$\tau_{22} = \lambda p_0 + \lambda \sqrt{\lambda} p_1 z_1, \quad |z_1| \le a/\sqrt{\lambda}, \quad z_2 = 0$$
(20a)

$$u_2 = 0, \quad |z_1| > a/\sqrt{\lambda}, \quad z_2 = 0$$
 (20b)

$$\tau_{12} = 0, \quad |z_1| < \infty, \quad z_2 = 0 \tag{20c}$$

$$\tau_{11}, \tau_{22}, \tau_{12} \to 0, \quad \sqrt{z_1^2 + z_2^2} \to \infty$$
(20d)

The problem is first solved in the z_1 – z_2 plane and the final integral equation is transformed back to the physical z–x plane as follows (Jin and Mai 1997)

$$\frac{\lambda}{\pi\sqrt{2(1+\kappa)}} \int_{-1}^{1} \frac{\phi(s)}{s-r} ds = -\frac{1}{E_0} (p_0 + p_1 ar), \quad (21)$$

$$|r| \le 1$$

where r = z/a and $\phi(r)$ is the unknown density function defined by

$$\phi(z) = \frac{\partial u_x}{\partial z}|_{x=0} \tag{22}$$

The solution of Eq. (21) has the following form

$$\phi(r) = \frac{\psi(r)}{\sqrt{1 - r^2}} = \frac{\sqrt{2(1 + \kappa)}}{2\lambda E_0} \frac{1}{\sqrt{1 - r^2}} \left[p_0 \tilde{\psi}^{(0)}(r) + p_1 a \tilde{\psi}^{(1)}(r) \right]$$
(23)

Once the solution of the above integral equation is obtained, the stress intensity factors at the crack tips can be calculated from

$$K_{I}(a) = -\frac{1}{2}\sqrt{\pi a} \Big[p_{0}\tilde{\psi}^{(0)}(1) + p_{1}a\tilde{\psi}^{(1)}(1) \Big],$$

$$K_{I}(-a) = \frac{1}{2}\sqrt{\pi a} \Big[p_{0}\tilde{\psi}^{(0)}(-1) + p_{1}a\tilde{\psi}^{(1)}(-1) \Big]$$
(24)

Besides the stress intensity factor, the crack surface opening displacement is also an important physical quantity which can be calculated from

$$\delta(r) = -\frac{2a\sqrt{2(1+\kappa)}}{2\lambda E_0} \times \left[p_0 \int_r^1 \frac{\tilde{\psi}^{(0)}(s)}{\sqrt{1-s^2}} ds + p_1 a \int_r^1 \frac{\tilde{\psi}^{(1)}(s)}{\sqrt{1-s^2}} ds \right]$$
(25)

Using the Chebyshev polynomial expansion method, the solution of $\tilde{\psi}^{(0)}(r)$ and $\tilde{\psi}^{(1)}(r)$ can be found as

$$\tilde{\psi}^{(0)}(r) = -2T_1(r) = -2r, \quad -1 \le r \le 1$$

$$\tilde{\psi}^{(1)}(r) = -T_2(r) = 1 - 2r^2, \quad -1 \le r \le 1$$
(26)

where $T_1(r)$ and $T_2(r)$ are degree 1 and 2 Chebyshev polynomials of the first kind, respectively. The stress intensity factors at the upper and lower crack tips are found to be



$$K_I(a) = \left(p_0 + \frac{1}{2}p_1 a\right)\sqrt{\pi a},$$

$$K_I(-a) = \left(p_0 - \frac{1}{2}p_1 a\right)\sqrt{\pi a}$$
(27)

which are the same as those for isotropic materials. The crack opening displacement (COD) is

$$\delta(r) = \frac{a\sqrt{2(1+\kappa)}}{\lambda E_0} (2p_0 + p_1 ar)\sqrt{1-r^2}$$
 (28)

Substituting Eq. (27) into Eq. (19) yields the pressure parameters p_0 and p_1 as follows

$$p_0 = \frac{K_{lc}}{2\sqrt{\pi a}}, \quad p_1 = \frac{K_{lc}}{a\sqrt{\pi a}}$$
 (29)

Following Nakashima (1993) and Nunn (1996), the crack propagation velocity, V, is approximately determined using the following relationship based on the Poiseuille flow

$$V = \frac{\delta_{ave}^2}{12\eta} (\Delta \rho g - p_1) \tag{30}$$

where δ_{ave} is the average separation of the two crack surfaces (i.e., average fracture aperture) defined by

$$\delta_{ave} = \frac{1}{2a} \int_{-a}^{a} \delta(z)dz = \frac{a\sqrt{2(1+\kappa)}}{2\lambda E_0} p_0 \pi \tag{31}$$

and p_0 and p_1 given in Eq. (29). The velocity in Eq. (30) is also consistent with the first order approximation of fluid pressure in Eqs. (17) and (18) [with $\delta(0)$ replaced by $\delta_{\rm ave}$].

The critical crack length for upward buoyancy-driven propagation can be determined from Eqs. (30) and (29) using the condition V = 0, i.e.,

$$2a_c = 2\left(\frac{K_{lc}}{\Delta\rho g\sqrt{\pi}}\right)^{2/3} \tag{32}$$

which is the same as that for isotropic rocks given in Nunn and Meulbroek (2002).

4 Density and viscosity of methane gas

We consider methane gas in the numerical analysis. Both density and viscosity of methane gas are functions of pressure and temperature, which continuously vary during the upward vertical crack propagation. The density is generally determined using an equation of state (EOS) for the gas. The viscosity of the gas may be determined using some curve-fitting schemes.

An iterative approach is used to determine the gas density and the gas area which is also the crack area. It is always assumed that Eq. (19) is satisfied during crack propagation. For a given initial length of the crack at an initial depth (equal to or greater than the critical length), the crack volume (also the gas volume) can be determined using Eqs. (31) and (29) (we assume a unit crack width (1 m) in the plane of the blade crack in the calculation. The specific choice of the crack width does not influence the results of crack velocity and opening), and the average gas pressure in the crack can be determined using the excess pressure and confining pressure at the initial depth. The mole and hence mass of the gas is first calculated using the gas volume and pressure by the EOS. For a given upward crack extension measured from the crack center, a longer crack length is first assumed. The crack volume can then be calculated using Eq. (31), and the average gas pressure in the crack can be calculated using Eqs. (18) and (29), and the confining pressure. The average pressure thus calculated is subsequently used to determine the gas volume using the EOS. If the volumes determined from Eq. (31) and the EOS become equal (with a small tolerance), the computation is terminated for this crack propagation step and a new step is initiated. Otherwise, a new crack length is assumed based on the gas volume from the EOS and the computation continues until a converged volume is obtained. The density is finally determined using the volume and the mass of the gas (which is assumed as a constant during propagation).

4.1 An equation of state for methane gas

We employ an EOS developed by Duan et al. (1992) for methane gas. The EOS is valid over wide temperature and pressure ranges (0–1000 $^{\circ}$ C and 0–800 MPa, respectively). The P-V-T relation has the following form

$$\frac{P_r V_r}{T_r} = 1 + \frac{C_1}{V_r} + \frac{C_2}{V_r^2} + \frac{C_3}{V_r^4} + \frac{C_4}{V_r^5} + \frac{b_1}{V_r^2 T_r^3} \left(b_2 + \frac{b_3}{V_r^2}\right) \exp\left(-\frac{b_3}{V_r^2}\right)$$
(33)

where C_i (i = 1, 2, 3, 4) are



$$C_{1} = a_{1} + \frac{a_{2}}{T_{r}^{2}} + \frac{a_{3}}{T_{r}^{3}}, \quad C_{2} = a_{4} + \frac{a_{5}}{T_{r}^{2}} + \frac{a_{6}}{T_{r}^{3}},$$

$$C_{3} = a_{7} + \frac{a_{8}}{T_{r}^{2}} + \frac{a_{9}}{T_{r}^{3}}, \quad C_{4} = a_{10} + \frac{a_{11}}{T_{r}^{2}} + \frac{a_{12}}{T_{r}^{3}}$$
(34)

In Eqs. (33) and (34), $P_r = P/P_c$, $V_r = V/V_c$, $T_r = T/T_c$, P is the fluid pressure, V is the molar volume, T is the absolute temperature, P_c is the critical pressure required to liquefy methane at the critical temperature T_c , T_c is the critical temperature above which methane cannot be liquefied regardless of the pressure applied, $V_c = RT_c/P_c$, and R is the universal gas constant. The EOS contains 15 constants: a_i (i = 1, 2, ..., 12), and b_i (i = 1, 2, 3) which can be found in Duan et al. (1992).

4.2 Viscosity of methane gas

We employ the model by Sanjari et al. (2011) for methane gas. The model is valid for $0.01 < P_{\rm r} < 21$ and $1.01 < T_{\rm r} < 3.0$. The viscosity (in 0.1 μ Pa s) has the following form

$$\eta = \frac{\alpha_1 + \alpha_2 P_r + \alpha_3 P_r^2 + \alpha_4 \ln P_r + \alpha_5 \ln^2 P_r + \alpha_6 T_r^{-1} + \alpha_7 \ln^2 T_r}{1 + \alpha_8 P_r^2 + \alpha_9 T_r^{-1} + \alpha_{10} T_r^{-2} + \alpha_{11} T_r^{-3}}$$
(35)

where α_i (i = 1, 2, ..., 11) can be found in Sanjari et al. (2011).

5 Numerical results

This section presents numerical examples to illustrate effects of elastic anisotropy on the crack propagation/ fluid migration velocity and average crack opening (fracture aperture). In the numerical calculations, we consider water, oil and methane gas. The host rock has properties typical of shale (Nunn and Meulbroek 2002). Table 1 lists the material properties of the host rock and the physical properties of water and oil. The effect of elastic anisotropy is investigated by varying the modulus ratio, E_v/E_h with fixed E_h given in Table 1. The rock properties in the isotropic plane are assumed to be the same as those of the isotropic rock in all cases. In general anisotropic rocks, the fracture toughness also depends on orientation (Chen et al. 1998). For the vertical crack propagation in transversely isotropic rocks studied in this work, the fracture toughness in the isotropic (horizontal) plane is irrelevant and only the toughness for crack propagation in the vertical direction is needed. We use the fracture toughness data in Nunn (1996) and Nunn and Meulbroek (2002) for the source rock in the Gulf of Mexico. The crack is assumed to initiate at a depth of 4.0 km. The geothermal gradient is assumed to be 25 °C/km so that the initial temperature is 125 °C.

Figure 2 shows the propagation velocity of a water-filled crack versus crack length for both isotropic host rock and transversely isotropic rocks with $E_{\rm v}/E_{\rm h}=0.8$ and 1.2, respectively. Water compressibility is ignored so the crack area remains constant during propagation. The propagation velocity for the crack in the anisotropic rock with the smaller modulus ratio $(E_{\rm v}/E_{\rm h}=0.8)$ is more than 60% higher than that for the crack in the isotropic rock. For example, the velocity for the water-filled crack is about 0.33 mm/s for a 6.0 m long crack in the isotropic rock. The velocity increases to 0.55 mm/s for the anisotropic case. The propagation velocity for the crack in the anisotropic rock with the larger modulus ratio $(E_{\rm v}/E_{\rm h}=1.2)$,

Table 1 Properties of the host rock, water and oil (Nunn and Meulbroek 2002)

Young's modulus in the horizontal plane	$E_{\rm h}=2800~{\rm MPa}$
Poisson's ratio in the horizontal plane	$v_{hh} = 0.4$
Young's modulus in the vertical direction	$E_{\rm v} = 0.8E_{\rm h}, 1.2E_{\rm h}$
Poisson's ratio in the xz plane	$v_{hv} = 0.35, 0.45$
Shear modulus in the xz plane	$G_{\rm vh}=900~{\rm MPa}$
Density of rock	$\rho_{\rm rock} = 2300 \text{ kg/m}^3$
Fracture toughness in the vertical direction	$K_{\rm Ic} = 0.1 \text{ MPa m}^{1/2}$
Density of water	$\rho_{\rm water} = 1000 \text{ kg/m}^3$
Viscosity of water	$\eta_{\mathrm{water}} = 0.001 \; \mathrm{Pa} \; \mathrm{s}$
Density of oil	$\rho_{\rm oil} = 840 \text{ kg/m}^3$
Viscosity of oil	$\eta_{\rm oil} = 0.01 \; \mathrm{Pa} \; \mathrm{s}$



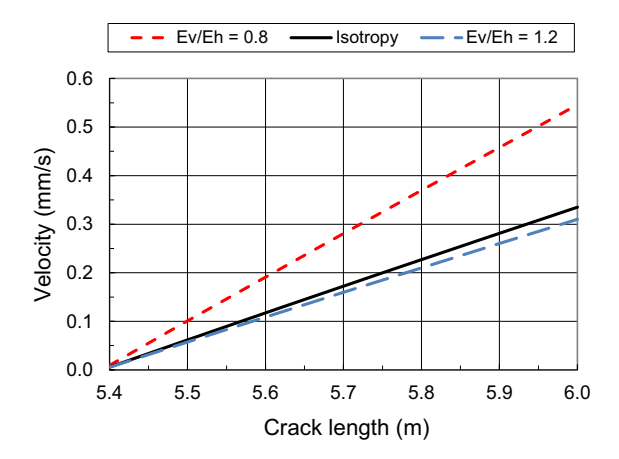


Fig. 2 Propagation velocity of a water-filled crack versus crack length for anisotropic rocks ($E_{\rm v}/E_{\rm h}=0.8$ and 1.2, $v_{\rm hv}=0.35$) and the corresponding isotropy medium

however, is slightly lower than that in the isotropic rock. The critical crack length for upward buoyancy-driven propagation is approximately 5.4 m according to Eq. (32). The crack can become longer than the critical length because it may intersect other water-filled cracks during upward propagation thereby trapping more fluid and increasing its length.

Figure 3 shows the average crack opening displacement (COD) (i.e., average fracture aperture) for a water-filled crack as a function of crack length for both isotropic host rock and transversely isotropic rocks with $E_{\rm v}/E_{\rm h}=0.8$ and 1.2, respectively. The COD for the anisotropic rock with the smaller modulus ratio $(E_{\rm v}/E_{\rm h}=0.8)$ is more than 25% larger than that for the

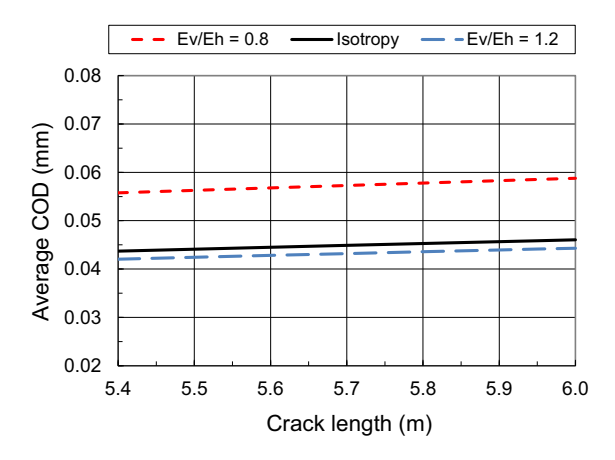


Fig. 3 Average fracture aperture (i.e., crack opening displacement) of a water-filled crack versus crack length for anisotropic rocks ($E_{\nu}/E_{h}=0.8$ and 1.2, $\nu_{h\nu}=0.35$) and the corresponding isotropy medium

isotropic rock. This explains the faster crack propagation velocity in the anisotropic rock shown in Fig. 2 because the propagation velocity is proportional to the square of the average COD according to Eq. (30). On the other hand, The COD for the anisotropic rock with the larger modulus ratio ($E_{\rm v}/E_{\rm h}=1.2$) is smaller than that for the isotropic rock.

The propagation velocity and the average COD for an oil-filled crack are shown in Figs. 4 and 5, respectively. The properties of the rocks are the same as those in Figs. 2 and 3. The compressibility of oil is also ignored. Similar to the water-filled crack, the propagation velocity and the average COD for the anisotropic rock with $E_{\rm v} < E_{\rm h}$ are significantly larger

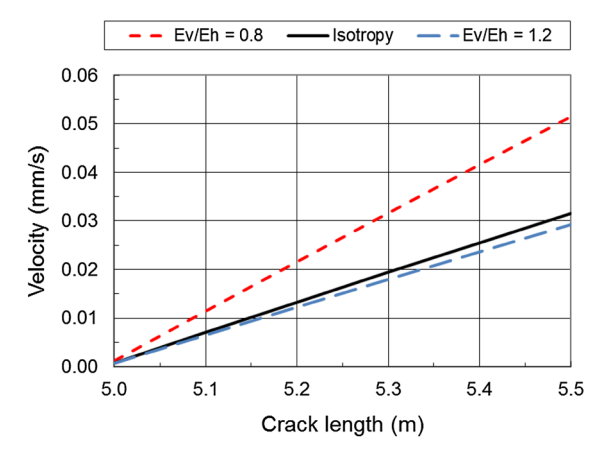


Fig. 4 Propagation velocity of an oil-filled crack versus crack length for anisotropic rocks ($E_{\rm v}/E_{\rm h}=0.8$ and 1.2, $\nu_{\rm hv}=0.35$) and the corresponding isotropy medium

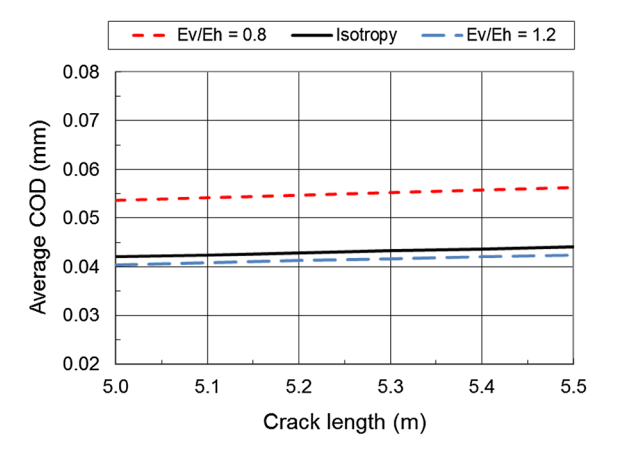


Fig. 5 Average fracture aperture (i.e., crack opening displacement) of an oil-filled crack versus crack length for anisotropic rocks ($E_v/E_h=0.8$ and 1.2, $v_{hv}=0.35$) and the corresponding isotropy medium



than the corresponding quantity for the isotropic rock, and propagation of the oil-filled crack is slower than that of the water-filled crack: oil has a higher viscosity and the propagation velocity is inversely proportional to the viscosity. The critical length for the oil-filled crack is approximately 5 m. As with water, the crack can become longer than the critical length because it may intersect other oil-filled cracks or pools during upward propagation. Finally, the propagation velocity and the average COD for the anisotropic rock with $E_{\rm v} > E_{\rm h}$ are smaller than the corresponding quantity for the isotropic rock.

As discussed in Sect. 3, for the linear fluid pressure distribution in Eq. (18) to be reasonably accurate for propagating cracks, the viscous flow induced pressure drop must be much smaller than the buoyancy force, i.e., $12\eta Va/\delta_{ave}^2 = 36a$ should be much smaller than $\Delta \rho ga$. We now examine if this condition is satisfied with water-filled and oil-filled cracks in the above examples with $E_{\rm v}/E_{\rm h}=0.8$. For a water-filled crack that is slightly longer than the critical length, i.e., 2a = 5.4 m, we have $\Delta \rho g a = 12753 a$ (g = 9.81 m/ s²) and $12\eta Va/\delta_{ave}^2 = 36a$. The condition is thus satisfied. For a crack length of 2a = 6 m, $12\eta Va/\delta_{ave}^2 = 1896a$, which indicates that the fluid pressure may be approximated by a linear function only for cracks that are not much longer than the length. For the oil-filled $\Delta \rho ga = 14323a$. For a crack length of 2a = 5.5 m, $12\eta Va/\delta_{ave}^2 = 1951a$, which also indicates that the linear fluid pressure may be reasonable.

Unlike the cases of water- and oil-filled cracks, the length of a gas-filled crack increases when it propagates towards the surface (Nunn and Meulbroek 2002). This is because the gas volume increases with decreasing pressure at shallower depths. Moreover, the critical length of a gas-filled crack for upward propagation depends on the depth. The critical length for a methane gas filled crack is about 4 m according to Eq. (32) and the gas density of 278 kg/m³ at the 4 km depth. Figure 6a shows the length evolution for a gas-filled crack during crack propagation. The crack has an initial length of 4.02 m, slightly longer than the critical length, at a depth of 4 km. The crack length increases from its initial value to about 4.65 m when the crack reaches a depth of 2 km. The modulus ratio $E_{\rm v}/E_{\rm h}$, however, does not affect the crack length variation. This is because both the stress intensity

factors (Eq. 27) and the critical crack length (Eq. 32) have the same expressions as those for isotropic rocks. For a transversely isotropic rock, the fracture toughness in the direction perpendicular to the isotropic plane is different from that in the isotropic plane. In this work we are mainly concerned with the effect of elastic anisotropy and assume that the fracture toughness for the corresponding isotropic rock has the same value as that in the direction perpendicular to the isotropic plane of the anisotropic rock.

Figure 6b, c shows the average density and viscosity of the gas in the crack during crack propagation. The density decreases from 278 kg/m³ at the initial 4 km depth to 224 kg/m³ when the crack reaches 2 km depth. The viscosity decreases from 42×10^{-6} Pa s at the 4 km depth to 30.5×10^{-6} Pa s at the 2 km depth. Again, the density and viscosity are not influenced by the modulus ratio.

Figure 7 shows the average COD versus depth during propagation of a gas-filled crack with an initial length of 4.02 m (slightly longer than the critical length). The COD also increases when the crack continuously propagates upward. For the isotropic host rock, the average COD increases from 0.038 mm at 4 km depth to 0.041 mm when the crack reaches 2 km depth. Compared with the isotropic rock case, the crack in the anisotropic rock with $E_{\rm v} < E_{\rm h}$ has a larger average COD, and that in the anisotropic rock with $E_{\rm v} > E_{\rm h}$ has a lower average COD. With increasing crack length and average COD in the anisotropic rock with $E_{\rm v} < E_{\rm h}$, the cross-sectional area of the blade crack also increases when the crack propagates to a shallower depth.

Figure 8 shows the propagation velocity for a gasfilled crack with an initial length of 4.02 m. The propagation velocity increases as the crack propagates upward. This is because the average fracture aperture and density difference become larger and the viscosity becomes smaller at shallower depths, which results in higher velocities as indicted by Eq. (30). For the isotropic rock, the velocity increases from 0.016 mm/s at the initial depth of 4 km to 17.5 mm/s when the crack propagates to a depth of 2 km. For the anisotropic rock cases, the velocity reaches 28.5 and 16.2 mm/s at a depth of 2 km for $E_{\rm v}/E_{\rm h}=0.8$ and 1.2, respectively.

The effect of Poisson's ratio v_{hv} in the xz plane on the propagation velocity is examined in Fig. 9. We consider a gas-filled crack with an initial length of 4.02 m at an initial depth of 4 km. The modulus ratio



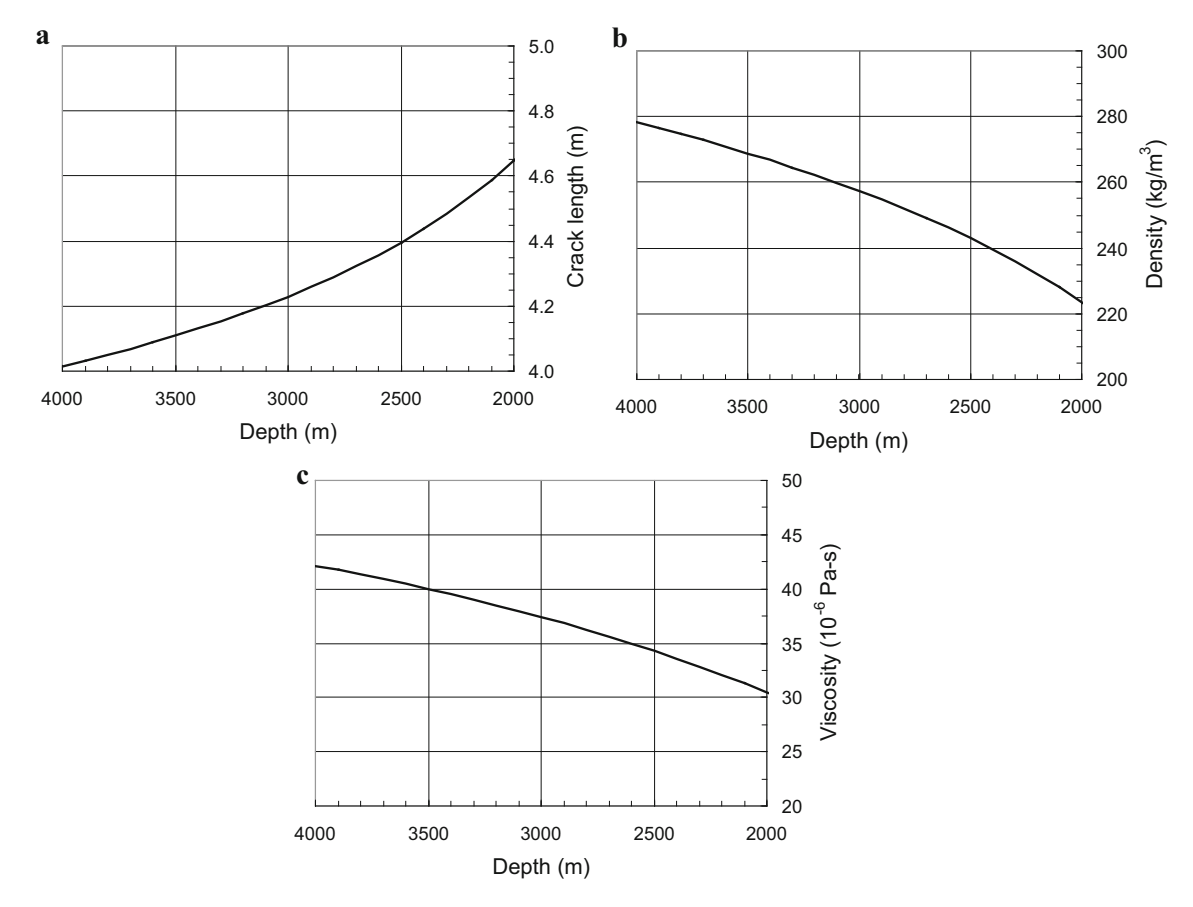


Fig. 6 a Length of a gas-filled crack versus depth as the crack continuously propagates upward (initial crack length =4.02 m). **b** Average density of the gas in the crack versus depth as the crack continuously propagates upward

(initial crack length = 4.02 m). c Average viscosity of the gas in the crack versus depth as the crack continuously propagates upward (initial crack length = 4.02 m)

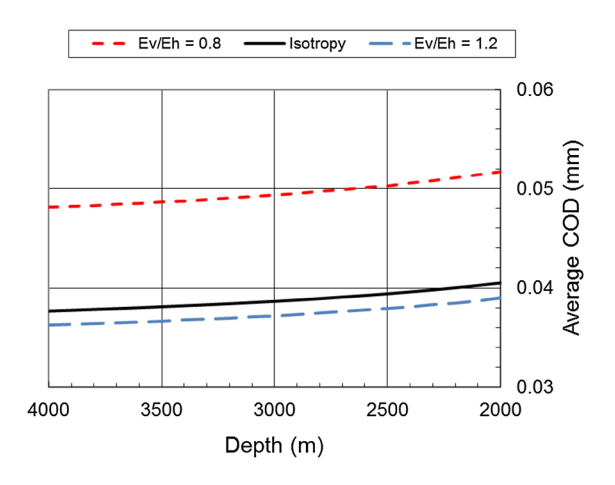


Fig. 7 Average fracture aperture (i.e., crack opening displacement) of a gas-filled crack versus depth for two values of anisotropy parameter $E_{\rm v}/E_{\rm h}$ and $v_{\rm hv}=0.35$ (initial crack length = 4.02 m)

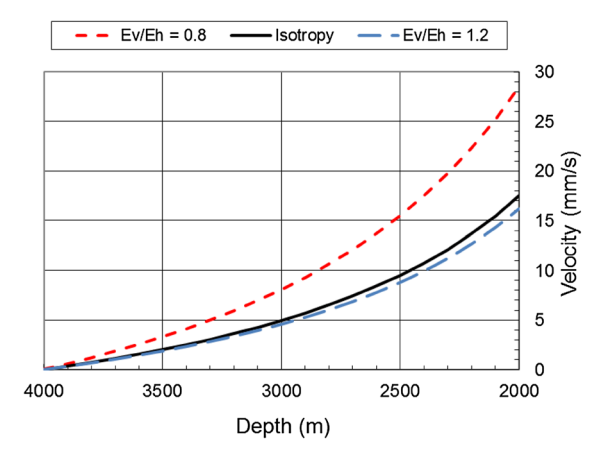


Fig. 8 Propagation velocity of a gas-filled crack versus depth for two values of anisotropy parameter $E_{\rm v}/E_{\rm h}$ and $v_{\rm hv}=0.35$ (initial crack length = 4.02 m)



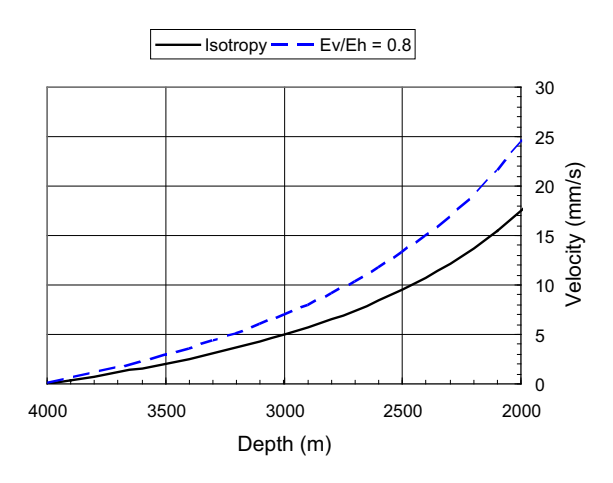


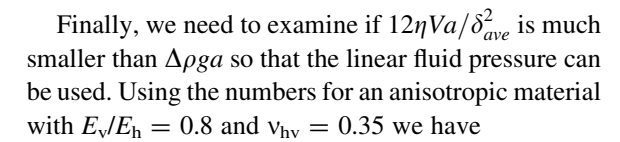
Fig. 9 Propagation velocity of a gas-filled crack versus depth for an anisotropic rock $(E_{\rm v}/E_{\rm h}=0.8,\ v_{\rm hv}=0.45)$ and the corresponding isotropy medium. The crack has an initial length of 4.02 m

is taken as $E_{\rm v}/E_{\rm h}=0.8$. We use a Poisson's ratio $v_{\rm hv}=0.45$, which is larger than that in the isotropic plane ($v_{\rm hh}=0.4$). The propagation velocity in the anisotropic rock is still much higher than that in the isotropic rock. However, the increase in velocity is less significant compared with the case of $v_{\rm hv}=0.35$ ($< v_{\rm hh}=0.4$) shown in Fig. 8.

It is generally accepted that Poiseuille flow equations can be used to describe flow of liquid (e.g., magma, water and oil) in propagating fractures (Spence et al. 1987; Lister and Kerr 1991; Nakashima 1993; Rubin 1995; Nunn 1996; Roper and Lister 2007). For application of the Poiseuille equations to gas flow in a fracture, the Reynolds number should be carefully examined so that no turbulent flow occurs. Using the numbers for the 4.02 m long initial crack in an anisotropic material with $E_{\nu}/E_{h}=0.8$ and $\nu_{h\nu}=0.35$, the Reynolds numbers may be estimated as follows

$$\begin{aligned} \text{Re} &= \frac{\rho_{gas} v \delta_{ave}}{\eta} \approx \frac{278 \times 0.026 \times 10^{-3} \times 0.048 \times 10^{-3}}{42 \times 10^{-6}} \\ &\approx 0.008 \quad \text{at } 4000 \text{ m} \\ \text{Re} &= \frac{\rho_{gas} v \delta_{ave}}{\eta} \\ &\approx \frac{224 \times 0.028 \times 0.052 \times 10^{-3}}{31.5 \times 10^{-6}} \approx 10 \quad \text{at } 2000 \text{ m} \end{aligned}$$

which are much smaller than the experimentally measured critical Reynolds number of 1350 for turbulent plane Poiseuville flow to occur (Dou and Khoo 2011).



$$12\eta Va/\delta_{ave}^2 = 5.69a$$
, $\Delta \rho ga = 19836a$ at 4000 m
 $12\eta Va/\delta_{ave}^2 = 3914a$, $\Delta \rho ga = 20366a$ at 2000 m

The above results indicate that the linear fluid pressure may be a reasonable approximation for the crack that has not reach 2000 m depth. At shallower depths, the viscous flow induced pressure drop will be a significant fraction of the buoyancy induced pressure, which may invalidate the use of the linear pressure distribution.

6 Approximations of fracture aperture using equations for isotropic materials

It is known from Sect. 2 that the transformed constitutive relation (10) using the equivalent elastic properties has the same form as that for isotropic rocks. An interesting question is whether or not approximate solutions of complex problems for anisotropic rocks can be obtained by employing the equations for isotropic materials together with the equivalent elastic properties. The advantage of this approach is that solutions of many problems of isotropic materials are available and they could be used as approximate solutions for anisotropic rocks by simply employing the equivalent properties. In this section, we explore this possibility in determination of the average fracture aperture.

For isotropic rocks with a modulus E and a Poisson's ratio v, the equivalent material constants in Eq. (8) reduce to

$$E_0 = \frac{E}{1 - v^2}, \quad v_0 = \frac{v}{1 - v}, \quad \lambda = 1, \quad \kappa = 1$$
 (36)

i.e., E_0 and v_0 represent the equivalent modulus and Poisson's ratio in plane strain. Using the above constants, the average fracture aperture in Eq. (31) reduces to

$$\delta_{ave}^{iso} = \frac{1 - v^2}{F} a p_0 \pi \tag{37}$$

An approximate average fracture aperture for transversely isotropic rocks may be formulated if we



adopt Eq. (37) for isotropic rocks and replace $(1 - v^2)/E$ by $1/E_0$, i.e.,

$$\delta_{ave}^{apr} = \frac{1}{E_0} a p_0 \pi \tag{38}$$

Now we examine the relative errors of using Eq. (38) to calculate the aperture. We also examine the error of using Eq. (37) with the modulus and Poisson's ratio in the isotropic plane of the transversely isotropic rock, i.e., E_h and v_{hh} for E and v_h respectively.

Using $E_v = 0.8E_h$ and the properties listed in Table 1 in Eq. (31) (precise anisotropy), Eq. (38) (approximate anisotropy) and Eq. (37) (isotropy with E_h and v_{hh}), we obtain

$$\delta_{ave} = 3.830 \times 10^{-4} a p_0 \pi,$$

 $\delta_{ave}^{apr} = 3.476 \times 10^{-4} a p_0 \pi,$
 $\delta_{ave}^{iso} = 3.000 \times 10^{-4} a p_0 \pi$

The relative errors for the approximate anisotropic and isotropic equations are 10.16 and 27.63%, respectively. If the modulus in the vertical direction increases to $E_{\rm v}=0.9E_{\rm h}$, the relative errors reduce to 8.48 and 17.68%, respectively. Finally, if we use $E_{\rm v}=0.8E_{\rm h}$ and a Poisson's ratio $v_{\rm hv}$ of 0.45 instead of 0.35, the relative errors become 5.32 and 17.61%, respectively. These results suggest that in some cases the formula for isotropic materials may be employed to approximately determine fracture aperture for transversely isotropic rocks by using the equivalent elastic constant E_0 of the anisotropic material.

7 Concluding remarks

Effects of material anisotropy on primary petroleum migration through buoyancy-driven propagation of an isolated blade crack filled by oil or gas are investigated. The host source rock is modeled as a linearly elastic, transversely isotropic medium which is described by an equivalent set of anisotropic elastic properties that, as far as we know, is new to the geophysics literature. We also assume steady state crack propagation and use a linear fluid pressure distribution in the crack (first order approximation of Poiseuille flow), which may be reasonably accurate for propagation of an isolated crack with a length equal to or slightly longer than the critical length. Our model

thus may be directly used to investigate migration of oil, gas and other fluids through transversely isotropic rocks and sediments with very low permeability. Parameters describing crack propagation and fluid migration velocity (stress intensity factors and crack opening displacement) are obtained by an integral equation method. In the case where the plane of transverse isotropy is horizontal, the numerical results show that (a) fluid transport velocity is significantly increased if the elastic modulus in the vertical direction is smaller than that in the horizontal direction. The velocity is slightly decreased if the elastic modulus in the vertical direction is larger than that in the horizontal direction, (b) the length of a gas-filled crack increases as the crack propagates from deeper to shallower levels in the crust and the elastic anisotropy does not influence this crack length increase, (c) the crack opening displacement (i.e., fracture aperture) and therefore velocity for a gas-filled crack increases as the crack propagates to shallower depths, and (d) at a given depth, the fracture aperture increases with a decrease in the elastic modulus in the vertical direction relative to that in the horizontal direction. Finally, in some cases the formula for isotropic materials may be employed to approximately determine fracture aperture for transversely isotropic rocks by using the equivalent elastic constant E_0 of the anisotropic material. Extension of this conclusion to more complex problems of anisotropic materials requires further investigation.

Acknowledgements This work was partly funded by NSF Grant EAR-1347087.

Compliance with ethical standards

Conflict of interest The author declares that they have no conflict of interest.

References

Amadei B, Pan E (1992) Gravitational stresses in anisotropic rock masses with inclined strata. Int J Rock Mech Min Sci Geomech Abstr 29:225–236

Bai T, Pollard DD (2001) Getting more for less: the unusual efficiency of fluid flow in fractures. Geophys Res Lett 28:65-68

Bayuk IO, Ammerman M, Chesnokov EM (2008) Upscaling of elastic properties of anisotropic sedimentary rocks. Geophys J Int 172:842–860



- Chen CS, Pan E, Amedei B (1998) Fracture mechanics analysis of cracked discs of anisotropic rock using the boundary element method. Int J Rock Mech Min Sci Geomech Abstr 35:195–218
- Chen Z, Jin ZH, Johnson SE (2007) A perturbation solution for dyke propagation in an elastic medium with graded density. Geophys J Int 169:348–356
- Comer JB, Hinch HH (1987) Recognizing and quantifying expulsion of oil from the Woodford Formation and age-equivalent rocks in Oklahoma and Arkansas. AAPG Bull 71:844–858
- Dahm T (2000a) Numerical simulations of the propagation path and the arrest of fluid-filled fractures in the earth. Geophys J Int 141:623–638
- Dahm T (2000b) On the shape and velocity of fluid-filled fractures in the earth. Geophys J Int 142:181–192
- Dou HS, Khoo BC (2011) Investigation of turbulent transition in plane Couette flows using energy gradient method. Adv Appl Math Mech 3:165–180
- Duan ZH, Moller N, Weare JN (1992) An equation of state for the CH_4 – CO_2 – H_2O system: I. Pure systems from 0 to 1000 °C and 0 to 8000 bar. Geochim Cosmochim Acta 56:2605–2617
- England WA, MacKenzie AS, Mann DM, Quigley TM (1987) The movement and entrapment of petroleum fluids in the subsurface. J Geol Soc Lond 144:327–347
- Hunt JM (1990) Generation and migration of petroleum from abnormally pressured fluid compartments. AAPG Bull 74:1–12
- Hunt JM (1996) Petroleum geochemistry and geology, 2nd edn. Freeman, San Francisco
- Jin ZH, Johnson SE (2008) Primary oil migration through buoyancy-driven multiple fracture propagation: oil velocity and flux. Geophys Res Lett 35:L09303
- Jin ZH, Mai YW (1997) Residual strength of an ARALL laminate containing a crack. J Compos Mater 31:746–761
- Jin ZH, Johnson SE, Cook AE (2015) Crack extension induced by dissociation of fracture-hosted methane gas hydrate. Geophys Res Lett 42:8522–8529
- Krenk S (1979) On the elastic constants of plane orthotropic elasticity. J Compos Mater 13:108–116
- Lash GG, Engelder T (2005) An analysis of horizontal microcracking during catagenesis: an example from the Catskill delta complex. AAPG Bull 89:1433–1449
- Law BE, Spencer CW (1998) Abnormal pressure in hydrocarbon environments. In: Law BE, Ulmishek GF, Slavin VI (eds) Abnormal pressures in hydrocarbon environments:
 AAPG memoir 70. American Association of Petroleum Geologists, Tulsa, pp 1–11
- Lister JR (1991) Steady solutions for feeder dykes in a densitystratified lithosphere. Earth Planet Sci Lett 107:233–242
- Lister JR, Kerr RC (1991) Fluid-mechanical models of crack propagation and their application to magma transport in dykes. J Geophys Res 96:10049–10077
- Mann U (1990) Sedimentological and petrophysical aspects of primary petroleum migration pathways. In: Förstner U,

- Heling D, Koch R, Rothe P, Stoffers P (eds) Sediments and environmental geochemistry—selected aspects and case histories. Springer, Heidelberg, pp 152–178
- Miller TW (1995) New insights on natural hydraulic fractures induced by abnormally high pore pressure. AAPG Bull 79:1005–1018
- Nakashima Y (1993) Buoyancy-driven propagation of an isolated fluid-filled crack in rock: implication for fluid transport in metamorphism. Contrib Miner Petrol 114:289–295
- Nelson RA (2001) Geological analysis of naturally fractured reservoirs, 2nd edn. Gulf Professional Publishing, Butterworth-Heinemann, Boston
- Nihei KT, Nakagawa S, Reverdy F, Myer LR, Duranti L, Ball G (2011) Phased array compaction cell for measurement of the transversely isotropic elastic properties of compacting sediments. Geophysics 76:WA113–WA123
- Nunn JA (1996) Buoyancy-driven propagation of isolated fluidfilled fractures—implications for fluid transport in Gulf of Mexico geopressured sediments. J Geophys Res 101:2963–2970
- Nunn JA, Meulbroek P (2002) Kilometer-scale upward migration of hydrocarbon in geopressured sediments by buoyancy-driven propagation of methane-filled fractures. AAPG Bull 85:907–918
- Palciauskas VV, Domenico PA (1980) Microfracture development in compacting sediments: relations to hydrocarbon maturation kinetics. AAPG Bull 64:927–937
- Pan E (1997) A general boundary element analysis of 2-D linear elastic fracture mechanics. Int J Fract 88:41–59
- Pan E, Amadei B (1996) Fracture mechanics analysis of 2-D cracked anisotropic media with a new formulation of the boundary element method. Int J Fract 77:161–174
- Pan E, Chen W (2015) Static green's functions in anisotropic media. Cambridge University Press, Cambridge
- Pan E, Yuan FG (2000) Boundary element analysis of threedimensional cracks in anisotropic solids. Int J Numer Methods Eng 48:211–237
- Pan PZ, Rutqvist J, Feng XT, Yan F (2014) TOUGH-RDCA modeling of multiple fracture interactions in caprock during CO₂ injection into a deep brine aquifer. Comput Geosci 65:24–36
- Roper SM, Lister JR (2007) Buoyancy-driven crack propagation: the limit of large fracture toughness. J Fluid Mech 580:359–380
- Rubin AM (1995) Propagation of magma-filled crack. Annu Rev Earth Planet Sci 23:287–3336
- Sanjari E, Lay EN, Peymani M (2011) An accurate empirical correlation for predicting natural gas viscosity. J Natl Gas Chem 20:654–658
- Spence DA, Sharp PW, Turcotte DL (1987) Buoyancy-driven crack propagation: a mechanism for magma migration. J Fluid Mech 174:135–153
- Weertman J (1971) Velocity at which liquid-filled cracks move in the Earth's crust or in glaciers. J Geophys Res 76:8544–8553

